Fermi National Accelerator Laboratory

FERMILAB-Conf-90/127-E
[E-665]

Xe/D_2 Cross-Section Ratio at Low x_{Bj} from Muon Scattering at 490 GeV/c *

The E665 Collaboration

presented by

Stephen R. Magill
University of Illinois at Chicago
Chicago, Illinois 60680

June 1990

* Presented at the 15th APS Division of Particles and Fields General Meeting (DPF '90), Houston, Texas, January 3-6, 1990.

Xe/D_2 Cross-section Ratio at Low x_{Bj} from Muon Scattering at 490 GeV/c

Stephen R. Magill
University of Illinois at Chicago
for the
E665 Collaboration at Fermilab[1]

Abstract

First measurements from the E665 experiment at Fermilab on the relative cross-sections of 490 GeV/c muons scattered from deuterium and xenon targets are presented. The scattered muons were in the kinematic range $Q^2 > 0.1(GeV/c)^2$ and very low x_{Bj} ($0.001 < x_{Bj} < 0.1$). Triggering on events in this kinematic region was accomplished with a special Small Angle Trigger which projected individual beam muons to form a veto region 30 meters from the target. Using this trigger, muons with scattered angles as small as 0.5 milliradians were detected.

1 E665 at FNAL

E665 at FNAL is the highest energy muon deep inelastic scattering experiment in the world. This experiment was designed to provide physics information on a variety of topics, including:

- Structure Functions and ratio of Structure Functions for nucleons and nuclei at low x_{Bj}.
- Current jet fragmentation with identified hadrons.
- Target jet fragmentation.
- Event structure relative to the virtual photon axis.
- Exclusive vector meson production.

The apparatus is shown in Figure 1 and includes the following features :

- E_μ from 100 GeV to 500 GeV.
- Open geometry with $\sim 4\pi$ hadron detection.
- Two large field volume superconducting dipole magnets.
- Particle identification system including Time-of-Flight, two Threshold Cerenkov Counters, and a Ring-Imaging Cerenkov Counter.
- Electromagnetic Calorimeter for neutral energy detection.
- Streamer Chamber vertex detector for the target fragmentation region.
- Independent scattered muon triggers based on minimum scattering angles of 0.5 mrad (Small Angle Trigger - SAT) and 3 mrad (Large Angle Trigger - LAT).
- Targets : Xenon (8.5 g/cm^2), Deuterium (16 g/cm^2), Hydrogen (7 g/cm^2).

The first data-taking period for this new apparatus began in July 1987 and ended in February 1988. For more information on the E665 apparatus, see reference [2].

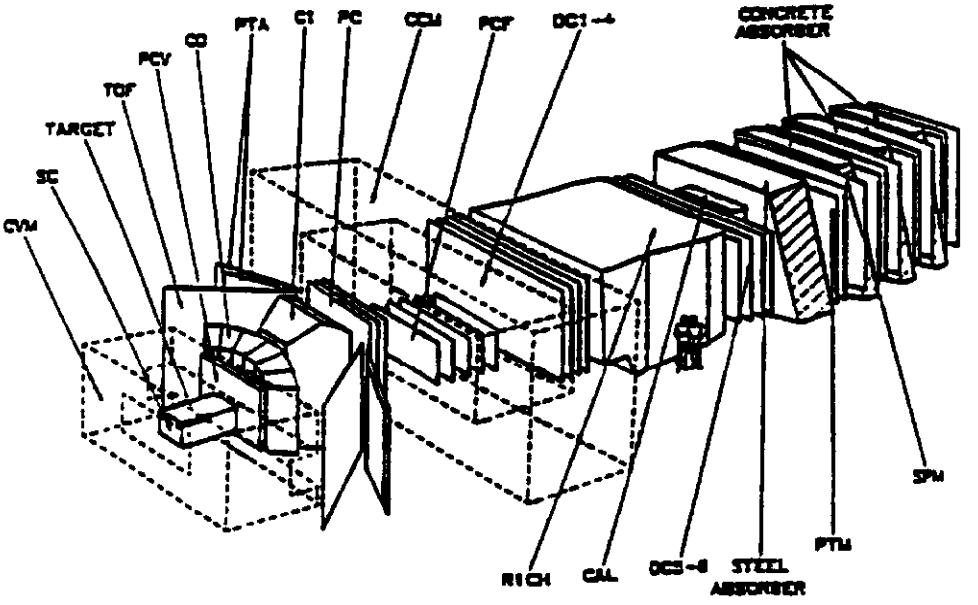

Figure 1: E665 Experimental Apparatus

2 Deep Inelastic Scattering Kinematics

Figure 2 shows the single virtual photon exchange Feynman diagram for muon-induced deep inelastic scattering. Included are the definitions and calculations of kinematical variables applicable in this analysis. The calculation of Q^2 includes the mass of the muon since the sample of low x_{Bj} is obtained at Q^2 down to 0.1 (GeV/c)^2.

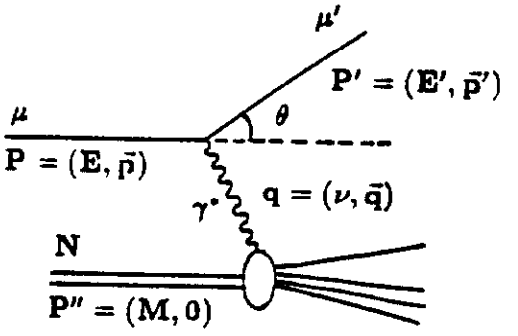

$$\nu = \mathrm{E} - \mathrm{E}'$$
$$\mathrm{Q}^2 = -\mathrm{q}^2 = -(\mathrm{P} - \mathrm{P}')^2$$
$$= -2\mathrm{m}_\mu^2 + 2\mathrm{E}\mathrm{E}' - 2|\vec{\mathrm{p}}||\vec{\mathrm{p}}'|\cos\theta$$
$$\mathrm{Y} = \nu/\mathrm{E}$$
$$\mathrm{x_{Bj}} = \frac{\mathrm{Q}^2}{2\mathrm{M}\nu}$$

Figure 2: DIS Single γ^* Exchange Diagram

The Feynman diagrams which represent radiative contributions to the muon vertex of order α^2 are shown in Figure 3. The vacuum polarization and vertex correction diagrams are target independent and so do not contribute to the total correction in the ratio of cross-sections. However, the diagrams corresponding to the bremsstrahlung process contribute in 3 different ways. The coherent process, in which the nucleus remains intact, and the quasi-elastic process, in which the nucleus breaks up into its constituent nucleons only, are strongly A dependent and, therefore, must be considered as corrections in the ratio of cross-sections. The inelastic contribution, in which the nucleon breaks up, depends in part on the structure function of the target nucleon, and is, therefore, weakly A dependent. In a heavy target, such as xenon, the coherent and quasi-elastic contributions dominate the total radiative correction at $y = \nu/E$ values greater than 0.5.

The contribution of the dominant radiative processes has been estimated by two independent

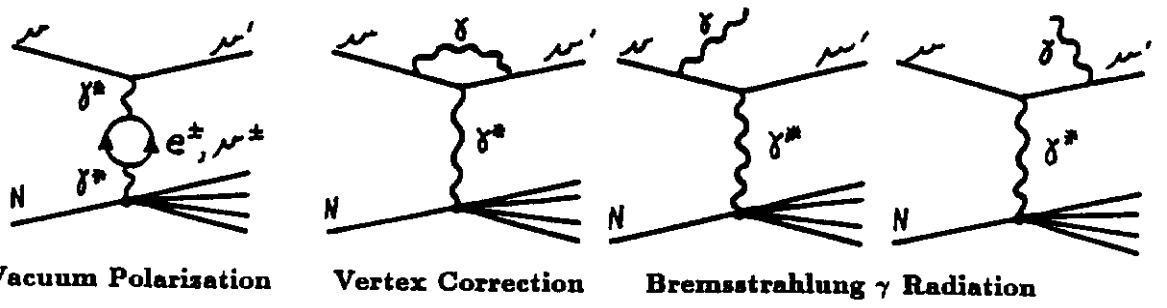

Figure 3: Radiative Corrections to Muon Vertex

methods : 1) a radiative correction Monte Carlo program based on an exact calculation [3]; and 2) use of the E665 electromagnetic calorimeter to eliminate radiative events from the deep inelastic scattered sample.

3 Event Sample - Kinematic Cuts

The distribution of events in the SAT trigger sample is shown in Figure 4. Note the position in the

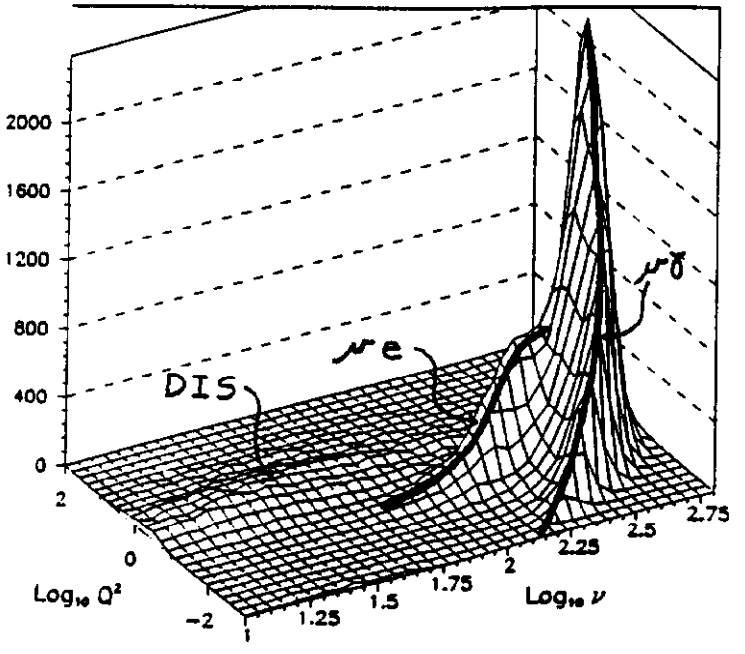

Figure 4: Log Q^2 vs Log ν Distribution of SAT Xenon Target Events

Q^2 vs ν event plane of the deep inelastic scatters, the elastic scattered μ - e events at constant x_{Bj}, and the μ - γ bremsstrahlung events primarily at high ν and low Q^2. The cuts used to define the current event sample are as follows : $Q^2 > 0.1\ (GeV/c)^2$; $\nu > 40\ GeV$; $x_{Bj} > 0.001$; $y < 0.75$; and are chosen to reduce the amount of electromagnetic background. In addition, a loose target position cut on the muon vertex was made.

4 Corrections and Systematic Errors

The data have been corrected for target acceptance, reconstruction efficiency of the scattered muon, empty target subtraction, and radiative events (unless the electromagnetic calorimeter was used to cut these events). Radiative corrections represent the largest correction to the raw ratio ($\sim$ 25% at $x_{Bj} = 0.001$). Using the electromagnetic calorimeter, E665 has been able to compare the results of radiative corrections from the two methods mentioned above, showing that they are consistent within statistical errors. The following table shows current estimates of the systematic errors due to the above corrections as well as from beam normalisation and target density.

Summary of Systematic Errors					
Source	**Estimate**	**Source**	**Estimate**	**Source**	**Estimate**
Beam Norm.	0.7 %	Trigger Acc.	2.8 %	MT Target Sub.	1.0 %
Target Density	0.4 %	Radiative Corr.	1.4 %	μ Recon.	4.0 %

5 Results

Figure 5 shows the ratio σ_{Xe}/σ_{D2} as a function of x_{Bj}. The data show that the cross-section per

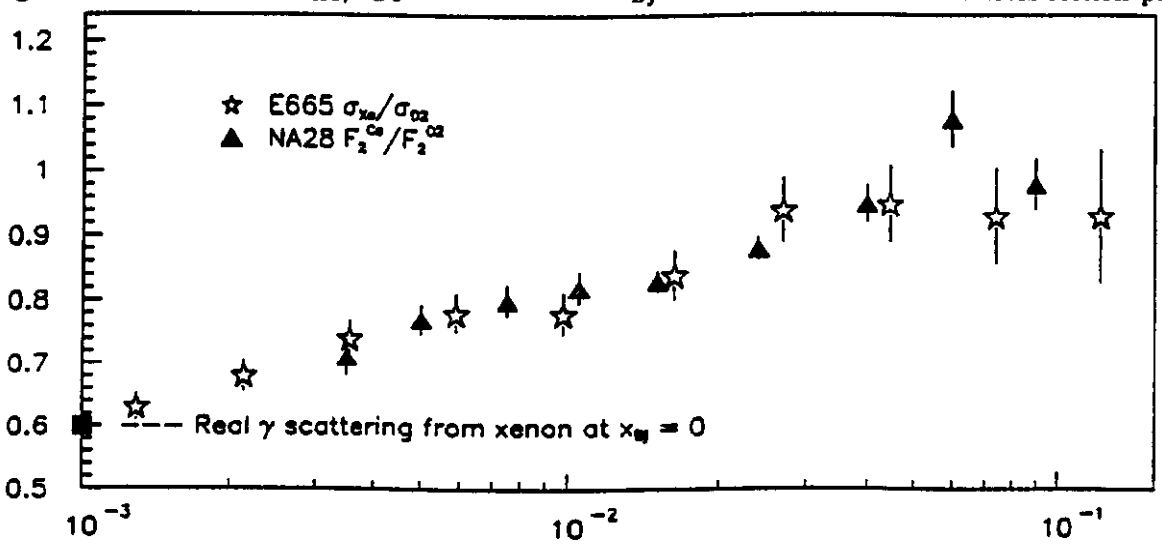

Figure 5: σ_A/σ_{D2} vs x_{Bj}

nucleon for muon scattering on Xe is suppressed relative to that for D_2 in the region $0.001 < x_{Bj} < 0.1$. This phenomena, called "shadowing", has been seen in γ - nucleus scattering at high energies [4] as well as in virtual photon scattering at low and high energies [5,6]. Recently, CERN experiment NA28 [6] has made measurements on carbon and calcium nuclei in much the same kinematic region as in this analysis. In Figure 5, data from E665 xenon and NA28 calcium are shown with statistical error bars only, indicating agreement between the two results in the shadowing region, and showing that E665 extends the kinematical range studied by NA28. Note that the data are consistent with an estimated real photon point (0.6 for xenon for $A^{eff} = 131^{0.9}$) [4].

In Figure 6, the Q^2 variation of σ_{Xe}/σ_{D2} for two x_{Bj} regions is presented with a comparison of NA28 calcium data. Once again, only statistical error bars are shown. The E665 data significantly extend the Q^2 range, and show that there is no Q^2 dependence of the σ_{Xe}/σ_{D2} ratio. This behavior indicates that the shadowing phenomenon observed is not consistent with naive vector dominance, but rather with models which predict shadowing as a result of parton recombination in heavy nuclei at low x_{Bj} [7] or with generalized vector dominance models [8].

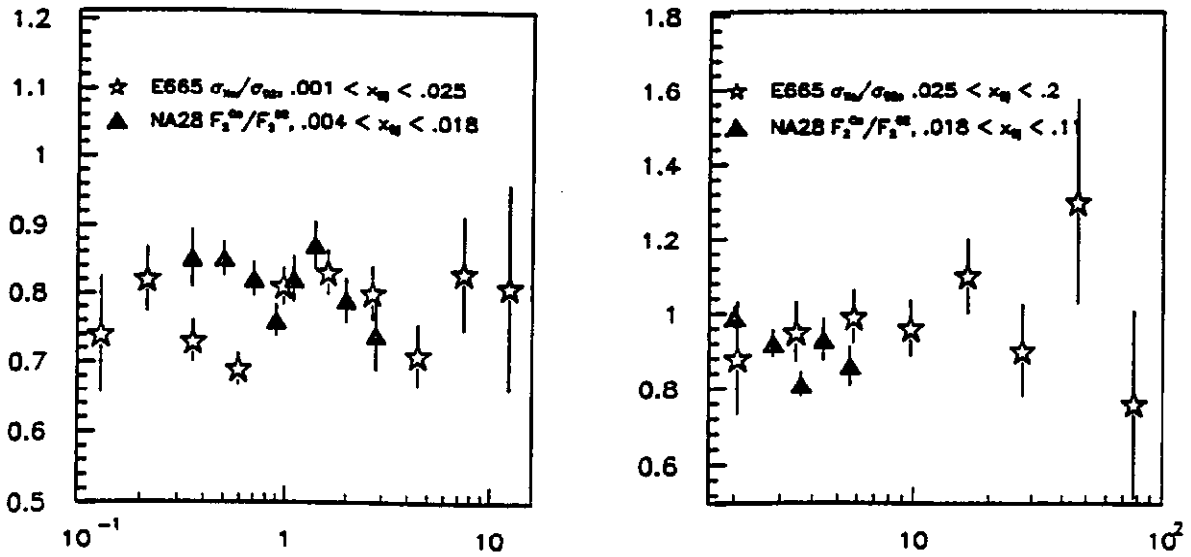

Figure 6: σ_A/σ_{D2} vs Q^2

6 Conclusion

In conclusion, the following points can be made from this analysis :

- Shadowing is seen in the ratio σ_{Xe}/σ_{D2} as a function of x_{Bj}.
- The dependence of σ_{Xe}/σ_{D2} on Q^2 is flat, indicating that the observed shadowing is of partonic origin. This is observed over the Q^2 range of $0.1 < Q^2 <\sim 30(GeV/c)^2$.

References

[1] Argonne, U.C. San Diego, Cracow, Fermilab, Freiburg, Harvard, U.I.C., Maryland, MIT, MPI Munich, Washington, Wuppertal, Yale.

[2] M. R. Adams, et. al.; FERMILAB-Pub-89/200-E;1989.

[3] L. W. Mo and Y. S. Tsai; Rev. Mod. Phys.; 41 (1969); Y. S. Tsai; SLAC-PUB-848; (1971).

[4] for example : D. O. Caldwell, et. al.; Phys. Rev. Lett.; 42 (1979).

[5] for example : J. Eickmeyer, et. al.; Phys. Rev. Lett.; 36 (1976).

[6] for example : M. Arneodo, et. al.; Nucl. Phys.; B333 (1990).

[7] F. E. Close, et. al.; Phys. Rev.; D40 (1989).

[8] for example : C. L. Bilchak, et. al.; Phys. Lett.; B214 (1988).